Biosensors and Bioelectronics ■ (■■■■) ■■■–■■■

Contents lists available at ScienceDirect

Biosensors and Bioelectronics

journal homepage: www.elsevier.com/locate/bios

Enhanced peroxidase-like activity of MoS_2/graphene oxide hybrid with light irradiation for glucose detection

Jian Peng, Jian Weng *

Department of Biomaterials, College of Materials, Xiamen University, Xiamen 361005, China

ARTICLE INFO

Article history:
Received 1 November 2015
Received in revised form
12 December 2015
Accepted 14 December 2015

Keywords:
MoS_2
Graphene oxide
Peroxidase-like
Synergistic interaction
Light
Glucose detection

ABSTRACT

Construction of novel enzyme-free mimetic is very important in improving the sensitivity of biosensor. Here, an intrinsic peroxidase-like activity of MoS_2 and graphene oxide (MoS_2/GO) hybrid is demonstrated and the hybrid is also used to detect glucose with high sensitivity. Firstly, the peroxidase-like activity of hydrid is compared with that of two components alone, the mixture of two components and horseradish peroxidase. The results show that the hydrid has highest catalytic activity and the Michaelis constant of this hybrid is 4.35 times lower and the maximal reaction velocity is 3.34 times higher than those of horseradish peroxidase, respectively. Electrochemical technologies are used to investigate the enhancing mechanism. The results show that the excellently catalytic performance could be attributed to the fast electron transfer on the surface of MoS_2/GO and the synergistic interaction of two components. Secondly, the effect of visible light and near-infrared light on the peroxidase-like activity of hybrid is also investigated. The results show that the limit of detection for H_2O_2 can be reduced from 10 nM to 2.5 nM with visible light. Thirdly, the hybrid is further used to detect glucose in serum with and without light. The results show that the hybrid has high selectivity and sensitivity for glucose detection in serum and the limit of detection for glucose is reduced from 0.83 μM to 65 nM with visible light. Therefore, the hybrid may have a potential application in glucose detection in serum with high sensitivity and selectivity.

1. Introduction

Enzyme-mimicking nanomaterials exhibit high stability against harsh reaction conditions. Meanwhile, they also have the following advantages: low cost in preparation and storage, flexibility in structure design, and tunable catalytic activities. Therefore, recent attention has been paid to the construction and discovery of novel enzyme-free mimetics. Graphene oxide (GO), a two-dimensional (2D) single atomic layer of carbon atoms arranged in a honeycomb lattice, was reported the peroxidase-like activity (Qu et al., 2011; Song et al., 2010). Compared to traditional horseradish peroxidase (HRP), GO is low-cost, easy to prepare, more stable to biodegradation, and less vulnerable to denaturation. To further enhance the catalytic activity of GO, several graphene-based hybrids have been prepared (Geim and Grigorieva, 2013; Huang et al., 2014; Haigh et al., 2012; Hong et al., 2013; Zhao et al., 2015). Typically, Au, Pd and Pt nanoparticles (NPs) were used to prepare the hybrids (Lv and Weng, 2013; Tao et al., 2013). However, the high cost due to the use of noble metal limits their further applications. Replacing noble metals with metal oxide or sulfide nanostructures may decrease the cost. However, these preparation methods are relative complex (Nie et al., 2013; Xing et al., 2014). Therefore, it remains a challenge to prepare graphene-based enzyme mimics by a simple and convenient method with low cost.

Recently, attention has been focused on the other 2D nanomaterials (Acerce et al., 2015; Chhowalla et al., 2013; Wang et al., 2012; Zeng et al., 2011), including the transition metal dichalcogenides (e.g., MoS_2), due to their 2D layer structure analogous to graphene. MoS_2 nanosheets were also reported as enzyme mimics recently (Lin et al., 2014a, 2014b). The MoS_2-graphene hybrids have been fabricated and show new properties in sensing, photocatalytic and batteries (Chang and Chen, 2011; Loan et al., 2014; Xiang et al., 2012). To the best of our knowledge, peroxidase-like ability of MoS_2-graphene hybrids has not been investigated. Moreover, graphene was reported to promote photocatalytic performance of semiconductors (Tu et al., 2013). Therefore, peroxidase-like ability of MoS_2-graphene hybrids under light irradiation may be enhanced and should be further explored.

Here, a high peroxidase-like activity of MoS_2 and graphene oxide (MoS_2/GO) hybrid was reported. To the best of our knowledge, we discovered for the first time that visible and near-infrared lights irradiation could enhance the peroxidase-like activity of

* Corresponding author.
E-mail address: jweng@xmu.edu.cn (J. Weng).

http://dx.doi.org/10.1016/j.bios.2015.12.034
0956-5663/

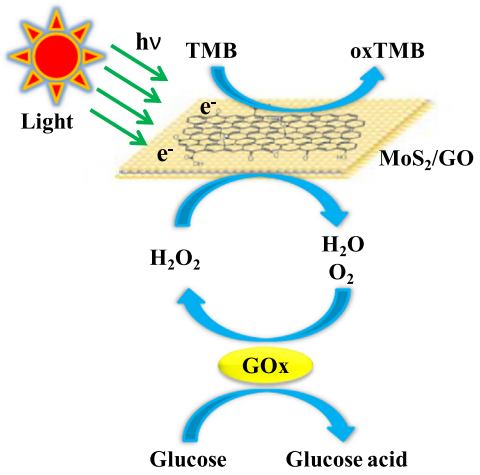

Scheme 1. Schematic illustration of glucose detection with glucose oxidase (GO*x*) and MoS_2/GO-catalyzed reactions under light irradiation.

hybrid. These excellent performances are attributed to the high electron transfer rate of MoS_2/GO and the synergistic interaction of two components. The hybrid was further applied to detect glucose in human serum samples with high sensitivity and selectivity (Scheme 1).

2. Materials and methods

2.1. Materials

Natural graphite powders (320 mesh) were purchased from Tianjin Guangfu chemical agent Co., Ltd. (Tianjin, China). MoS_2 (7–11 μm) was purchased from Alfa Aesar (Tianjin, China). H_2O_2 was purchased from Xilong Chemical (Guangzhou, China). Fructose, lactose, maltose, glucose and glucose oxidase (GO*x*) were purchased from Shanghai Sangon Biological Engineering Technology & Services Co., Ltd (Shanghai, China). 2,2′-azino-bis(3-ethylbenzthiazoline-6-sulfonic acid) (ABTS), o-phenylenediamine (OPD) and 3,3′,5,5′-tetramethylbenzidine (TMB) were purchased from J&K Chemical Co. (Beijing, China). Other chemicals were purchased from Green Bird Science and Technology Development (Xiamen, China). All chemicals were used without further purification.

2.2. Peroxidase-like activity of MoS_2/GO under light irradiation

MoS_2/GO and few-layer MoS_2 exfoliated in poly(vinyl alcohol) (PVA) were prepared according to our previous reports (Peng and Weng, 2015; Sun et al., 2014). Catalytic experiments were performed using 10 μg mL^{-1} of MoS_2/GO in a reaction volume of 600 μL acetic acid-sodium acetate buffer solution (0.02 M, pH 4, 25 °C) with 600 μM TMB as substrate, or 10 mM H_2O_2, unless otherwise stated. The enhanced peroxidase-like activity of MoS_2/GO under light irradiation was carried out in a quartz cell (1.0 cm × 1.0 cm × 4.5 cm) in the presence of catalyst under the irradiation of visible light (300 W Xe lamp, 400–800 nm) or infrared light (500 W infrared ovens lamp, 800–2500 nm). The enhanced peroxidase-like activity was monitored at 652 nm by real time detection on a TU-1901 UV–vis spectrometer.

2.3. H_2O_2 detection

H_2O_2 detection was carried out as follows: 180 μL of TMB (2 mM), 120 μL of MoS_2/GO (50 μg mL^{-1}) stock solution were added to 300 μL of H_2O_2 with different concentrations. The mixed solution was used to perform the time course measurement at the wavelength of 652 nm.

2.4. Glucose detection

Glucose detection was performed as follows: a) 20 μL of 10 mg mL^{-1} GO*x* and 180 μL of glucose with different concentrations in 0.5 mL of 10 mM Na_2HPO_4 buffer (pH 7.0) were incubated at 37 °C for 30 min; b) 0.2 mL of 6 mM TMB, 0.5 mL of the MoS_2/GO stock solution (200 μg mL^{-1}) and 8.6 mL of 0.02 M acetic acid-sodium acetate buffer (pH 4) were added to the above glucose reaction solution (0.7 mL); c) the mixed solution was incubated at 37 °C for 60 min; d) 10 μL H_2SO_4 (20%, v/v) was added into the mixture to stop the reaction, and the absorbance of the mixture was recorded at 450 nm. In control experiments, 5 mM maltose, 5 mM lactose, and 5 mM fructose were used to instead of glucose, respectively.

The detection of glucose in serum samples was performed according to the reported method (Lin et al., 2014a) with slight modifications: 50 μL of serum sample was diluted with 50 μL water, and then 500 μL $Ba(OH)_2$ (0.11 mol L^{-1}) and 500 μL $ZnSO_4$ (0.0765 mol L^{-1}) were added. After centrifugation at 4000 rpm for 10 min, 200 μL of the supernatant solution was taken. The other detection procedure was the same as that of glucose detection in Na_2HPO_4 buffer. The concentrations of glucose in serum samples were also determined by standard GOD-POD method.

3. Results and discussion

3.1. Characterization of materials

The XRD pattern of MoS_2/GO indicates that bulk MoS_2 had been successfully exfoliated as we expected (Fig. S1a, Supplementary material). The as-obtained MoS_2/GO is a thin 2D flake according to the TEM images (Fig. S1b and c). Raman spectra show that the peak E^1_{2g} was blue-shifted after exfoliation (Fig. S1g), indicating that the few-layer MoS_2 with a thickness in the range of 1–3 layers had been successfully produced (Eda et al., 2011). The peak at 224 nm is attributed to the π–π transition of GO. The peaks at 612 and 672 nm are due to exciton splitting with a separation of ~60 nm (~0.16 eV), which is characteristic of the 2H-MoS_2 phase (Winchester et al., 2014). The spectra also showed a broader absorption band from 400 to 455 nm (2.73 eV) after exfoliation, which can be due to the exfoliation of bulk MoS_2 into nanosheets with a thickness of several nanometers. The C, O, Mo and S elements uniformly distribute in sheets (Fig. S2), indicating that there is a strong interaction between GO and few-layer MoS_2 to form the MoS_2/GO hydrid. Few-layer MoS_2 exfoliated in PVA (MoS_2) was also characterized well (Fig. S3).

3.2. Peroxidase-like activity

To assess the peroxidase-like activity of the MoS_2/GO, TMB–H_2O_2 reaction is used as a model reaction because coloress TMB can be oxidized to a color product in the presence of catalyst (Fig. S4b). Fig. 1a shows that the absorbance of TMB oxidation product is increased with time in the mixture of TMB, H_2O_2 and MoS_2/GO. Fig. 1b demonstrates that both of H_2O_2 and as-obtained MoS_2/GO can not alone oxidize TMB efficiently to produce a blue color. Therefore, TMB oxidation is resulted from the decomposition of H_2O_2 by as-obtained MoS_2/GO. To further characterize the peroxidase-like activity of the MoS_2/GO, other two peroxidase substrates, ABTS and OPD, were used to replace TMB (Fig. S4a). All results confirm that the as-prepared MoS_2/GO exhibits an intrinsic peroxidase-like activity similar to HRP. Fig. 1c compares the

Please cite this article as: Peng, J., Weng, J., Biosensors and Bioelectronics (2015), http://dx.doi.org/10.1016/j.bios.2015.12.034

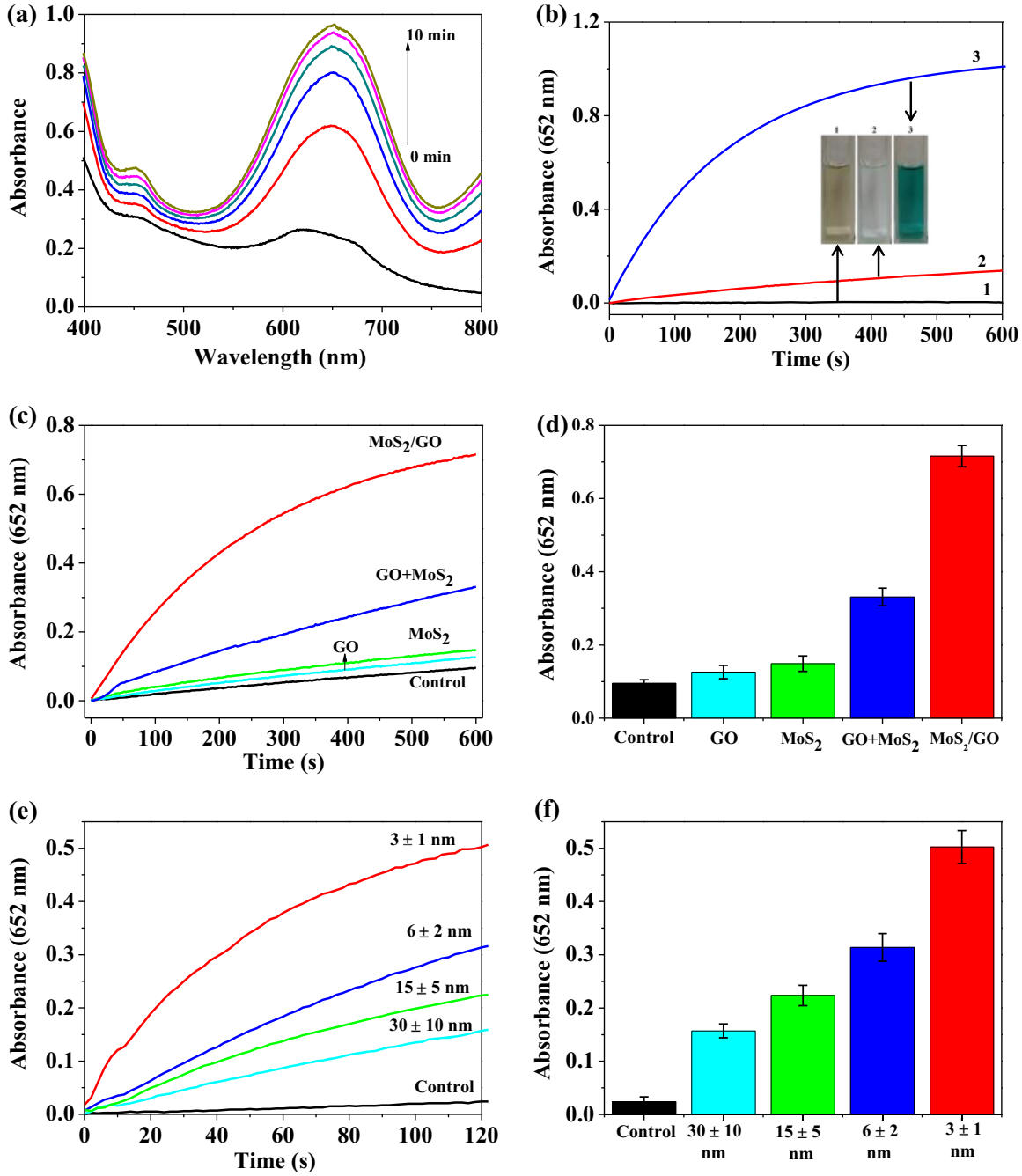

Fig. 1. Peroxidase-like activity of MoS_2/GO. (a) UV–vis spectra of the mixed solution of TMB, H_2O_2 and MoS_2/GO with time increasing. (b) The time-dependent absorbance changes at 652 nm of TMB solutions in the presence of MoS_2/GO (1), H_2O_2 (2), MoS_2/GO and H_2O_2 (3), respectively; Inset is the photograph of above three solutions after 10 min. (c) The time-dependent absorbance changes at 652 nm of TMB solutions in the presence of GO, MoS_2, simple mixing of two components (GO+MoS_2) and MoS_2/GO, respectively. (d) The absorbance in (c) after reaction for 10 min. (e) The time-dependent absorbance change at 652 nm of TMB in the presence of MoS_2/GO with different thickness. (f) The absorbance in (e) after reaction for 2 min. Three replicates were performed.

catalytic activity of GO, MoS_2, simple mixing of two components (GO+MoS_2) and MoS_2/GO. This experiment was performed according to the following steps. First, the contents of GO (57.2 wt%) and MoS_2 (42.8 wt%) in MoS_2/GO were calculated according to TGA data (Fig. S5 and Table S1). Then a simple mixing of two components (GO+MoS_2) is obtained by only mixing of 57.2 wt% GO and 42.8 wt% MoS_2 in solution which the final concentration is same as MoS_2/GO. At last, the catalytic properties of 57.2 wt% GO and 42.8 wt% MoS_2 were investigated, respectively. Obviously, the absorbance at 652 nm for MoS_2/GO (Fig. 1d) has the highest value than that of addition of two components alone or simple mixing of two components. In addition, the absorbance at 652 nm for mixing of two components (GO+MoS_2) is a little higher than that of the addition for GO and MoS_2 alone, which is due to a weak synergy when two components are simply mixed. The result shows that there might be strongly synergistic effect of two components to improve the catalytic activity of MoS_2/GO. MoS_2/GO with different thciknesses were prepared and characterized well in our previous work (Peng and Weng, 2015) and their XPS spectra and data were also listed in Fig. S6 and Table S2. The absorbance at 652 nm in Fig. 1e and f shows a thickness-dependent manner and the thinner MoS_2/GO has higher value than that of thicker one, which might be attributed to the better conductivity of thinner MoS_2 (Wang et al., 2013a). The optimal pH, temperature, and H_2O_2

Please cite this article as: Peng, J., Weng, J., Biosensors and Bioelectronics (2015), http://dx.doi.org/10.1016/j.bios.2015.12.034

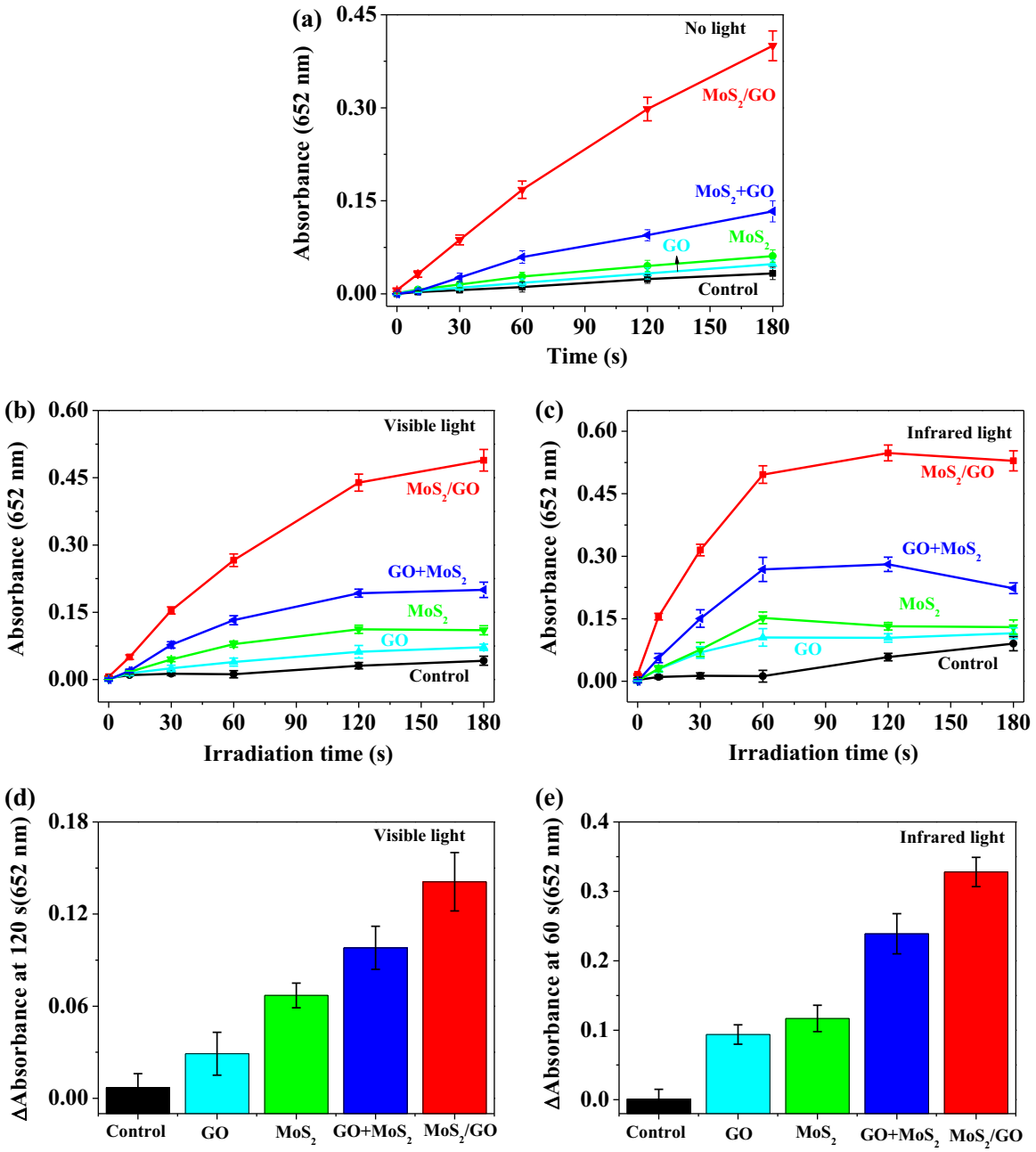

Fig. 2. Peroxidase-like activity of as-prepared nanomaterials under light irradiation. Absorbance change at 652 nm at different intervals for the mixed solution of TMB and H_2O_2 in the presence of different catalysts without light (a), under visible (b) and infrared (c) lights irradiation. (d) The absorbance change in (b) after irradiation for 120 s under visible light. (e) The absorbance change in (c) after irradiation for 60 s under infrared light. Three replicates were performed.

concentration (Fig. S7a–c) are 4.0, 37 °C and 200 mM, respectively, which is almost the same as these values for natural enzyme HRP. Fig. S7d demonstrates that the reaction rate increases with the MoS_2/GO concentration increasing and reaches a plateau at 10 μg mL^{-1}.

3.3. *Mechanism of peroxidase-like activity*

Fig. S8 shows the absorption and fluorescence change in the mixed solution of MoS_2/GO, methylene blue (MB) or terephthalic acid (TA), and H_2O_2. Compared with control experiments, the absorbance of MB was obviously decreased and the fluorescence intensity at 435 nm was remarkably enhanced, which indicates the presence of ·OH radicals (Jv et al., 2010; Satoh et al., 2007; Ishibashi et al., 2000). The enzyme kinetics experiments of MoS_2/GO with H_2O_2 and TMB as substrates were further carried out in order to understand the catalytic mechanism and acquiring kinetic parameters. A series of experiments were performed by changing the concentration of one substrate and fixing the concentration of another (Fig. S9a and d). The typical Michaelis–Menten curves (Fig. S9b and e) and Lineweaver–Burk plots (Fig. S9c and f) can be obtained and the important kinetic parameters such as K_m and V_{max} can be derived (Table S3). The apparent K_m value of MoS_2/GO with H_2O_2 as the substrate is 25.6 times lower than that of hemin (Lv and Weng, 2013), 770 times lower than that of Fe_3O_4 magnetic nanoparticles and 18.5 times lower than that of HRP (Gao et al., 2007). The V_{max} of MoS_2/GO with H_2O_2 and TMB as the substrates is 2.26 and 3.34 times higher than that of HRP, respectively, which could be attributed to the synergetic effect between GO and MoS_2. Thus, MoS_2/GO indeed shows a higher peroxidase-like activity

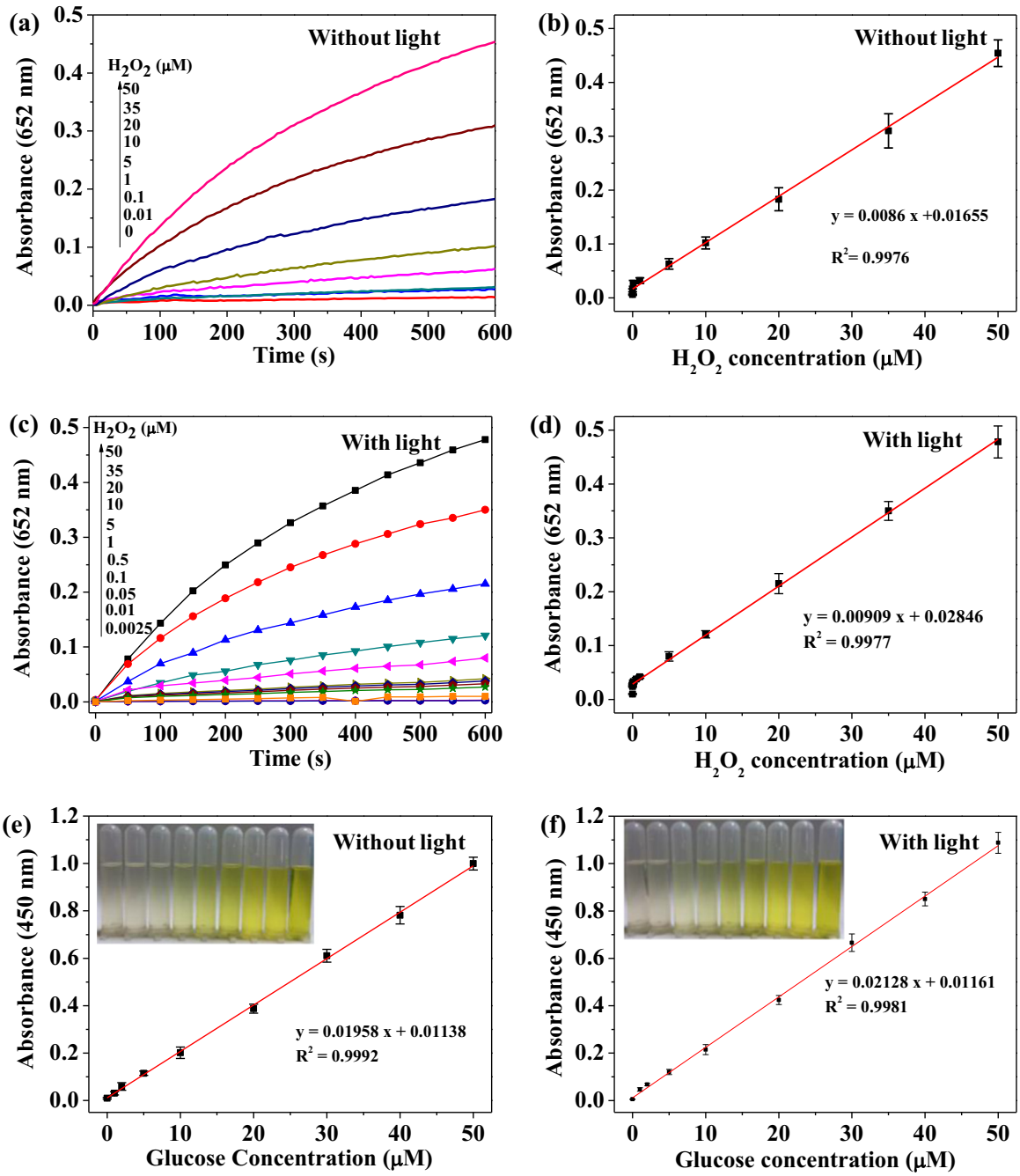

Fig. 3. Detection of H_2O_2 and glucose with or without visible light. The time-dependent absorbance changes at 652 nm with different concentrations of H_2O_2 without (a) and with (c) visible light. (b, d) Linear calibration plot for H_2O_2 calculated from (a) and (c), respectively. The linear calibration plots for glucose detection without (e) and with (f) visible light. Inset: photographies of colored products in glucose with different concentrations. The concentration of glucose increases from 0 (left) to 50 μM (right). Three replicates were performed.

than that of natural enzyme HRP. The thermodynamics of H_2O_2 oxidation catalyzed by MoS_2/GO is investigated at different temperatures from 25 to 39 °C shown in Fig. S10. The calculated E_a (24.64 kJ mol^{-1}) is lower than other reported catalysts (Wang et al., 2013b; Huang et al., 2009; Hasnat et al., 2010; Ma et al., 2012), indicating a high catalytic activity for the as-prepared MoS_2/GO (Table S4).

Fig. S11a shows that MoS_2/GO-modified electrode has the highest current intensity and lowest peak-to-peak separation (MoS_2/GO is 88 mV, GO is 107 mV and MoS_2 is 162 mV) than that of others, indicating faster electron-transfer kinetics at MoS_2/GO-modified electrode than that of others (Weng et al., 2005). Fig. S11c indicates that thinner MoS_2/GO-modified electrode has higher current intensity than that of thicker one, further demonstrating thinner MoS_2/GO would have higher conductivity than that of thicker one. Fig. S11b shows the electrocatalytic activities of H_2O_2 by MoS_2/GO, MoS_2 and GO. Among three different electrodes, MoS_2/GO-modified electrode shows higher current intensity which also means that it had highest catalytic activity. We also investigated the electrocatalytic activity of H_2O_2 by MoS_2/GO with different thicknesses (Fig. S11d). Among different electrodes, the thinnest MoS_2/GO (3 ± 1 nm)-modified electrode shows the highest current intensity, which also means that it had highest catalytic activity toward H_2O_2. The result indicates faster electron-transfer kinetics at thinner MoS_2/GO-modified electrode than that of thicker one, which might be the reason for the higher catalytic

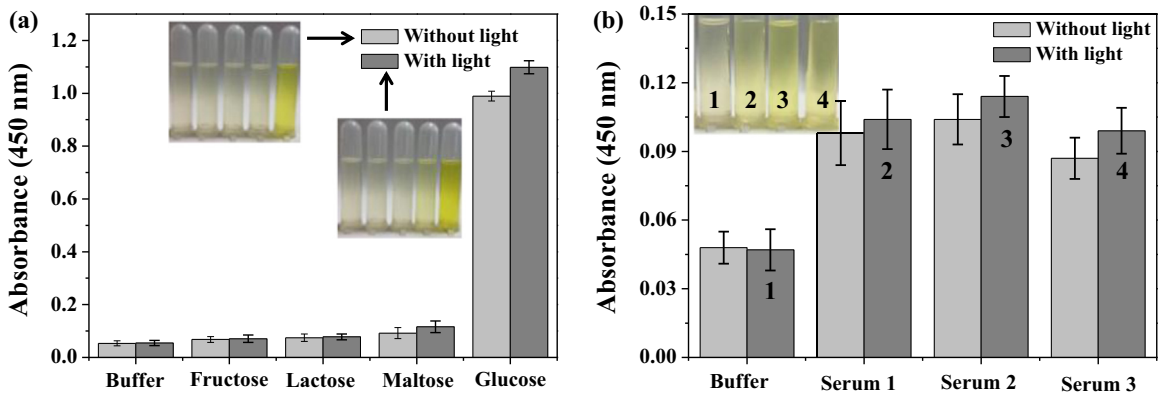

Fig. 4. (a) Selective detection of glucose with or without visible light. Insert: photographies of oxidized products in 5 mM fructose, 5 mM lactose, 5 mM maltose and 1 mM Glucose. (b) Detection of glucose in human serum with or without visible light. Insert: photographies of products after glucose oxidation in serum samples with visible light. Three replicates were performed.

activity of thinner MoS_2/GO than that of thicker one. Higher surface area of MoS_2/GO (0.050 cm^2) in Fig. S12 indicates that it would have higher conductivity than that of MoS_2 (surface area: 0.033 cm^2) and GO (surface area: 0.017 cm^2).

3.4. Peroxidase-like activity with light irradiation

To investigate the peroxidase-like activity of MoS_2/GO with light irradiation and further understand the synergetic effect between GO and MoS_2, UV–vis spectra at different intervals under the same condition were collected to compare the effect of different catalysts under visible or infrared light irradiation. Fig. 2 compares the enhanced catalytic activity of MoS_2/GO, simple mixing of two components and two components alone under irradiation in visible or infrared light. Fig. 2a shows that an obvious synergistic effect of two components in MoS_2/GO could be observed to improve the catalytic activity without light. In the presence of visible light irradiation (Fig. 2b), absorbance at 652 nm experiences an obviously increase from 0 to 120 s and the increase reaches a plateau at 120 s. The absorbance at 652 nm for MoS_2/GO at 120 s (Fig. 2d) has the higher value than that of addition of two components alone or simple mixing of two components. The result shows the synergistic effect really could be achieved under visible light irradiation. Meanwhile, the similar result can be obtained under infrared light irradiation (Fig. 2c and e). The reaction is much quicker under infrared light irradiation and reaches a plateau at 60 s. The amount of H_2O_2 oxidation at 120 s under visible light irradiation is 1.5 times of that without light and the amount of H_2O_2 oxidation at 60 s under infrared light irradiation is 3.3 times of that without light. The result indicates that visible and infrared lights not only accelerate the catalytic reaction, but also improve the amount of H_2O_2 oxidation. The control experiments in Fig. 2b–e indicate that there is no obvious absorbance change for the mixture of TMB and H_2O_2 without catalyst under irradiation of visible and infrared lights. The result further demonstrates that visible and infrared lights would promote the synergistic effect of two components in MoS_2/GO to improve its photocatalytic activity.

3.5. Application to H_2O_2 detection

On the basis of intrinsic and enhanced peroxidase-like property of MoS_2/GO in the absence and presence of light, we developed a simple colorimetric method to detect H_2O_2. The concentration response curve of H_2O_2 to the absorbance of TMB in the absence of light is presented in Fig. 3a. A linear relationship is established in the range of 0.1–50 μM with a correlation coefficient of 0.9976 (Fig. 3b). The detection limit of H_2O_2 is about 10 nM (the signal-to-noise ratio is two). As the intrinsic peroxidase-like property of MoS_2/GO could be further enhanced under light irradiation, as an example, visible light is chosen to investigate H_2O_2 detection. The concentration response curve of H_2O_2 to the absorbance of TMB in the presence of visible light is presented in Fig. 3c. A linear relationship is established in the range of 0.05–50 μM with a correlation coefficient of 0.9977 (Fig. 3d). The detection limit of H_2O_2 is decreased to about 2.5 nM (the signal-to-noise ratio is two), which is lower than that of many other nonenzymatic sensors (Table S5).

In order to further check the practical application of MoS_2/GO, it is used to determine H_2O_2 concentration in three real water samples. Good recovery and precision of H_2O_2 determination suggest that the peroxidase-like activity-based colorimetric method might be used to analyze H_2O_2 in real water samples (Table S6).

3.6. Application to glucose detection

H_2O_2 is the main product of a GO*x*-catalyzed reaction of glucose oxidation. When combined with GO*x* (Scheme 1), the proposed colorimetric method could be used for the determination of glucose. The linear range for glucose detection is from 1 to 50 μM (R^2=0.9992) with a detection limit of 0.83 μM without light (Fig. 3e) and 86 nM under visible light (the signal-to-noise ratio is two), which is lower than that of many other nonenzymatic sensors (Table S7). The result shows that MoS_2/GO would be a sensitively artificial enzyme and the sensitivity could be improved by light. Generally, the serum glucose concentrations in healthy and diabetic individuals range from 3–8 mM to 9–40 mM, respectively (Xu et al. 2007). After diluting the serum samples, the proposed method could be applied to detect glucose in serum.

Fructose, lactose, and maltose were used to investigate the selectivity of this biosensing system. Fig. 4a demonstrates that the absorbance of oxidized products from these glucose analogs (5 mM) is negligible compared with that of glucose (1 mM) with or without visible light. This indicates that this biosensing system would have high selectivity for glucose, which could be attributed to the high affinity of glucose oxidase for glucose. The application of this biosensing system to different serum samples and the photographies of oxidized products in serum samples are illustrated in Fig. 4b. We could clearly see the yellow color for serum samples compared to buffer (Fig. 4b insert) and visible-light can also enhance the absorbance of each serum sample. According to the calibration curve, the concentrations of glucose in the normal human serum samples measured by this method agreed well with that measured by standard GOD-POD method (Table S8). The

results indicate that this biosensing system might have a potential application in detection of glucose in real serum samples.

4. Conclusion

In conclusion, we have demonstrated that MoS_2/GO possesses intrinsic and light-enhanced peroxidase-like activity and its catalytic activity for decomposition of H_2O_2 is higher than that of other reported catalysts and HRP. The high catalytic activity of MoS_2/GO could be attributed to its high conductivity and the synergistic interaction of two components. On this basis, we constructed a simple, sensitive and selective colorimetric assay to detect H_2O_2 and glucose in serum samples with or without visible light. MoS_2/GO, as novel peroxidase mimetic, shows several advantages over natural enzymes and other existing alternatives, such as easy preparation, low cost and light-enhanced activity, and may have a potential application in medical diagnostics, environmental monitoring and photocatalysis.

Acknowledgment

This work is supported by the National Key Scientific Research Projects (2014CB932004), National Natural Science Foundation of China (31371005, 81171453), the Fundamental Research Funds for the Central Universities and Scientific and Technological Innovation Platform of Fujian Province of China (2014H2006).

Appendix A. Supplementary material

Supplementary data associated with this article can be found in the online version at http://dx.doi.org/10.1016/j.bios.2015.12.034.

References

Acerce, M., Voiry, D., Chhowalla, M., 2015. Nat. Nanotechnol. 10, 313–318.
Chang, K., Chen, W.X., 2011. ACS Nano 5, 4720–4728.
Chhowalla, M., Shin, H.S., Eda, G., Li, L.J., Loh, K.P., Zhang, H., 2013. Nat. Chem. 5, 263–275.
Eda, G., Yamaguchi, H., Voiry, D., Fujita, T., Chen, M.W., Chhowalla, M., 2011. Nano Lett. 11, 5111–5116.
Gao, L.Z., Zhuang, J., Nie, L., Zhang, J.B., Zhang, Y., Gu, N., Wang, T.H., Feng, J., Yang, D. L., Perrett, S., Yan, X., 2007. Nat. Nanotechnol. 2, 577–583.
Geim, A.K., Grigorieva, I.V., 2013. Nature 499, 419–425.
Haigh, S.J., Gholinia, A., Jalil, R., Romani, S., Britnell, L., Elias, D.C., Novoselov, K.S., Ponomarenko, L.A., Geim, A.K., Gorbachev, R., 2012. Nat. Mater. 11, 764–767.
Hasnat, M.A., Rahman, M.M., Borhanuddin, S.M., Siddiqua, A., Bahadur, N.M., Karim, M.R., 2010. Catal. Commun. 12, 286–291.
Hong, Y.J., Yang, J.W., Lee, W.H., Ruoff, R.S., Kim, K.S., Fukui, T., 2013. Adv. Mater. 25, 6847–6853.
Huang, C.P., Huang, Y.F., Cheng, H.P., Huang, Y.H., 2009. Catal. Commun. 10, 561–566.
Huang, X., Tan, C.L., Yin, Z.Y., Zhang, H., 2014. Adv. Mater. 26, 2185–2204.
Ishibashi, K., Fujishima, A., Watanabe, T., Hashimoto, K., 2000. Electrochem. Commun. 2, 207–210.
Jv, Y., Li, B.X., Cao, R., 2010. Chem. Commun. 46, 8017–8019.
Lin, T.R., Zhong, L.S., Guo, L.Q., Fu, F.F., Chen, G.N., 2014a. Nanoscale 6, 11856–11862.
Lin, T.R., Zhong, L.S., Song, Z.P., Guo, L.Q., Wu, H.Y., Guo, Q.Q., Chen, Y., Fu, F.F., Chen, G.N., 2014b. Biosens. Bioelectron. 62, 302–307.
Loan, P.T.K., Zhang, W.J., Lin, C.T., Wei, K.H., Li, L.J., Chen, C.H., 2014. Adv. Mater. 26, 4838–4844.
Lv, X.C., Weng, J., 2013. Sci. Rep. 3, 3285–3294.
Ma, Y., Meng, S., Qin, M., Liu, H., Wei, Y., 2012. J. Phys. Chem. Solids 73, 30–34.
Nie, G.D., Zhang, L., Lu, X.F., Bian, X.J., Sun, W.N., Wang, C., 2013. Dalton Trans. 42, 14006–14013.
Peng, J., Weng, J., 2015. Carbon 94, 568–576.
Qu, F.L., Li, T., Yang, M.H., 2011. Biosens. Bioelectron. 26, 3927–3931.
Satoh, A.Y., Trosko, J.E., Masten, S.J., 2007. Environ. Sci. Technol. 41, 2881–2887.
Song, Y.J., Qu, K.G., Zhao, C., Ren, J.S., Qu, X.G., 2010. Adv. Mater. 22, 2206–2210.
Sun, L.P., Lin, Z.Q., Peng, J., Weng, J., Huang, Y.Z., Luo, Z.Q., 2014. Sci. Rep. 4, 4794–4802.
Tao, Y., Lin, Y.H., Huang, Z.Z., Ren, J.S., Qu, X.G., 2013. Adv. Mater. 25, 2594–2599.
Tu, W.G., Zhou, Y., Zou, Z.G., 2013. Adv. Funct. Mater. 23, 4996–5008.
Wang, Q.H., Kalantar-Zadeh, K., Kis, A., Coleman, J.N., Strano, M.S., 2012. Nat. Nanotechnol. 7, 699–712.
Wang, T.Y., Zhu, H.C., Zhuo, J.Q., Zhu, Z.W., Papakonstantinou, P., Lubarsky, G., Lin, J., Li, M.X., 2013a. Anal. Chem. 85, 10289–10295.
Wang, Z.B., Lv, X.C., Weng, J., 2013b. Carbon 62, 51–60.
Weng, J., Xue, J.M., Wang, J., Ye, J.S., Cui, H.F., Sheu, F.S., Zhang, Q.Q., 2005. Adv. Funct. Mater. 15, 639–647.
Winchester, A., Ghosh, S., Feng, S.M., Elias, A.L., Mallouk, T., Terrones, M., Talapatra, S., 2014. ACS Appl. Mater. Interfaces 6, 2125–2130.
Xiang, Q.J., Yu, J.G., Jaroniec, M., 2012. J. Am. Chem. Soc. 134, 6575–6578.
Xing, Z.C., Tian, J.Q., Asiri, A.M., Qusti, A.H., Al-Youbi, A.O., Sun, X.P., 2014. Biosens. Bioelectron. 52, 452–457.
Xu, Y., Pehrsson, P.E., Chen, L.W., Zhang, R., Zhao, W., 2007. J. Phys. Chem. C. 111, 8638–8643.
Zeng, Z.Y., Yin, Z.Y., Huang, X., Li, H., He, Q.Y., Lu, G., Boey, F., Zhang, H., 2011. Angew. Chem. Int. Ed. 50, 11093–11097.
Zhao, H., Dong, Y.M., Jiang, P.P., Wang, G.L., Zhang, J.J., 2015. ACS Appl. Mater. Interfaces 7, 6451–6461.

Please cite this article as: Peng, J., Weng, J., Biosensors and Bioelectronics (2015), http://dx.doi.org/10.1016/j.bios.2015.12.034